in the supernatants of HIV-infected T cells can activate normal T cells to mobilize calcium in the absence of gp120-specific antibody. This discrepancy cannot be resolved at present. We have tested two different preparations of gp120 (one of which is a fusion protein) and obtained the same results with both. However, unlike Kornfeld *et al.* (*6*), we did not use supernatants of HIV-infected T cells as a source of gp120. In agreement with the findings presented here, Ledbetter *et al.* (*11*) showed that a monoclonal antibody to CD4 inhibits anti-CD3–mediated Ca_i^{2+} mobilization in resting T cells when CD4 is cross-linked before the administration of anti-CD3. We have confirmed this observation with WT/31. These studies suggest that ligation and cross-linking of CD4 downregulates T cell function before the T cell receptor is engaged.

Whether or to what extent gp120-specific antibodies contribute to establishing immunodeficiency in HIV-infected individuals cannot be determined from our results. It appears conceivable that gp120 disseminated by HIV-replicating cells forms bloodborne complexes with anti-gp120, thus exposing noninfected CD4-bearing T cells to continuous downregulatory signals that may eventually lead to immunodeficiency of the kind seen in mice after treatment with anti-CD4. The exquisite efficacy of gp120–anti-gp120 complexes in inhibiting T cell receptor–mediated calcium flux may also be viewed as favorable to a gp120-mediated autoimmune mechanism. It places this regulatory phenomenon in a dose range of contributory reagents (gp120 and anti-gp120) that can reasonably be expected to occur in HIV-infected individuals.

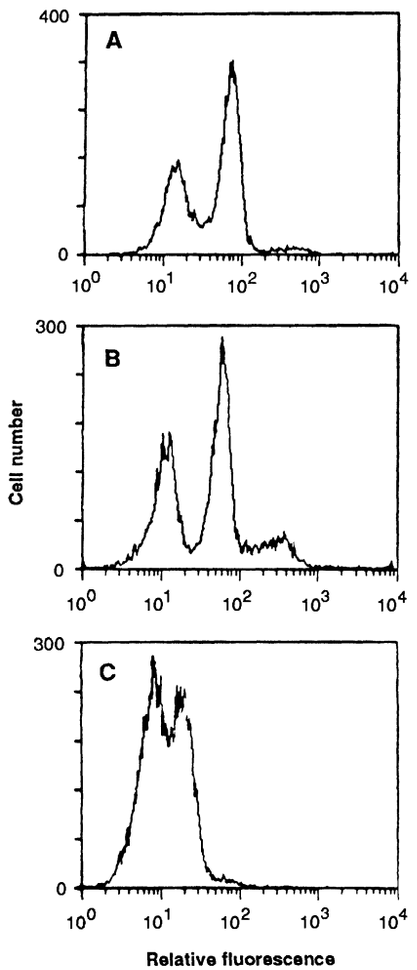

Fig. 3. Modulation of CD4 on the T cell surface by gp120–anti-gp120. (**A**) T cells treated with gp120 (150 μg/ml) were immediately exposed to IgG from AIDS patients (30 μg/ml) and fluorescein isothiocyanate–conjugated second antibody. (**B**) The gp120-treated T cells were incubated for 2 hours at 37°C before anti-gp120 and second antibody were added. (**C**) The gp120-treated T cells were incubated for 2 hours with anti-gp120 before the fluoresceinated second antibody was added.

REFERENCES AND NOTES

1. B. E. Bierer, B. P. Sleckman, S. E. Ratnofsky, S. D. Burakoff, *Annu. Rev. Immunol.* **7**, 579 (1989).
2. S. Stober, *Immunol. Today* **7**, 153 (1986).
3. D. Klatzman *et al.*, *Nature* **312**, 767 (1984).
4. J. S. McDougal, *Science* **231**, 382 (1986).
5. P. J. Maddon *et al.*, *Cell* **47**, 333 (1986).
6. H. Kornfeld *et al.*, *Nature* **355**, 445 (1988).
7. P. C. Diamond *et al.*, *J. Immunol.* **141**, 3715 (1988).
8. A. P. Fields, D. Bednarik, A. Hess, W. Stratford-May, *Nature* **333**, 278 (1988).
9. H. Spits *et al.*, *J. Immunol.* **135**, 1922 (1985).
10. R. S. Mittler, unpublished data.
11. J. A. Ledbetter *et al.*, *Eur. J. Immunol.* **18**, 525 (1988).
12. G. Gandernack, T. Leivestad, J. Ugelstad, E. Thorsby, *J. Immunol. Methods* **90**, 179 (1986).
13. P. S. Rabinowitch, C. H. June, A. Grossmann, J. A. Ledbetter, *J. Immunol.* **137**, 952 (1986).

14. We thank K. Small, K. Budzko, and D. Armstrong for providing us with patient sera, and H. F. Oettgen and S. Koenig for their comments on the manuscript. Recombinant gp120 preparations were kindly provided by Genetic Systems and by Genentech. We thank B. Forbes for manuscript preparation.

21 June 1989; accepted 7 August 1989

Mutant Potassium Channels with Altered Binding of Charybdotoxin, a Pore-Blocking Peptide Inhibitor

RODERICK MACKINNON* AND CHRISTOPHER MILLER

The inhibition by charybdotoxin of A-type potassium channels expressed in *Xenopus* oocytes was studied for several splicing variants of the *Drosophila Shaker* gene and for several site-directed mutants of this channel. Charybdotoxin blocking affinity is lowered by a factor of 3.5 upon replacing glutamate-422 with glutamine, and by a factor of about 12 upon substituting lysine in this position. Replacement of glutamate-422 by aspartate had no effect on toxin affinity. Thus, the glutamate residue at position 422 of this potassium channel is near or in the externally facing mouth of the potassium conduction pathway, and the positively charged toxin is electrostatically focused toward its blocking site by the negative potential set up by glutamate-422.

CHARYBDOTOXIN (CTX) IS A 37–amino acid peptide found in the venom of the scorpion *Leiurus quinquestriatus*. This peptide inhibits, at nanomolar concentrations, several types of K^+-specific ion channels, including Ca^{2+}-activated K^+ channels from many vertebrate tissues (*1*), *Aplysia* neurons (*2*), and red blood cells (*3*), and voltage-dependent K^+ channels from lymphocytes (*4*). The molecular mechanism by which CTX inhibits K^+ channels is understood. The peptide inhibitor binds to the channel with one-to-one stoichiometry, and physically occludes its outer "mouth," thus blocking K^+ permeation through the pore. This conclusion emerged from mechanistic studies on the high-conductance Ca^{2+}-activated K^+ channel from rat skeletal muscle, reconstituted into planar lipid bilayers (*5*). Potassium ions moving through the channel pore from the internal solution can destabilize CTX on its blocking site (*6*) and tetraethylammonium ion, which blocks the channel pore from the external solution, competitively prevents CTX from binding (*7*).

Charybdotoxin also inhibits the A-type K^+ channel coded by the *Shaker* gene of *Drosophila melanogaster* expressed in *Xenopus* oocytes (*8*). CTX inhibition of this K^+ channel is mechanistically similar to the peptide's effects on the well-studied Ca^{2+}-activated K^+ channel. Since cDNA clones of the *Drosophila* K^+ channel have been isolated (*9*), it is a good candidate for a detailed molecular investigation of the CTX-channel interaction. We therefore examined the CTX inhibition of four natural variants within the

Howard Hughes Medical Institute, and Graduate Department of Biochemistry, Brandeis University, Waltham, MA 02254.

*Present address: Department of Cellular and Molecular Physiology, Harvard Medical School, Boston, MA 02115.

Shaker K^+ channel family, as well as of several site-directed mutants of this channel.

Because the Shaker K^+ channel protein has not been purified, we have no direct information about its membrane folding structure. Therefore, our approach to the identification of a CTX binding region involved some initial guesswork. We were guided by two pieces of information. First, the strong homology between this K^+ channel and the voltage-dependent Na^+ channel (*10*) leads to a plausible transmembrane folding model (Fig. 1). This model is similar to those proposed by several groups (*10, 11*), and it suggests regions of the protein that may be exposed to the external solution. Second, we know that in the case of the Ca^{2+}-activated K^+ channel, the interaction between CTX and the ion channel is strongly electrostatic: negatively charged groups close to the outer mouth favor the binding of the cationic toxin (*5, 12*). This result suggests that aspartate or glutamate residues on the channel are involved in toxin binding.

We studied the effect of CTX on four naturally occurring splicing variants of Shaker, Sh A, B, C, and D (*13–15*), in hopes of finding different blocking characteristics. These channels share an identical "core" sequence, which is flanked by variable amino and carboxyl termini (Fig. 1). However, we found no significant differences among these four natural variants (*16*). Therefore, we used site-directed mutagenesis as a strategy to search for residues contributing to CTX binding. Because of the strongly electrostatic nature of the CTX-channel interaction, we focused on negatively charged residues as targets for mutagenesis. We replaced acidic with neutral residues located in the putative external loops (Fig. 1) and observed the effect of these alterations on CTX block of K^+ currents. Four mutations of a total of seven acidic residues in two of the proposed external loops have no effect on CTX inhibition (Fig. 2); the toxin inhibition curves for these mutants precisely match that of the wild-type channel. Moreover, these data illustrate the excellent reproducibility of the CTX inhibition assay.

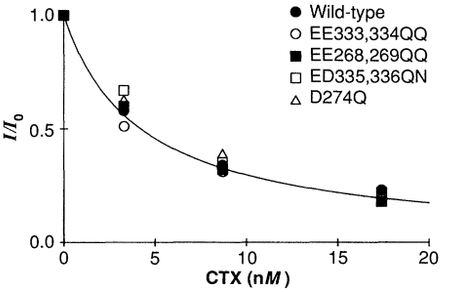

Fig. 2. Variations in channel structure that do not affect CTX block. K^+ currents were measured during depolarizing pulses from −100 mV to membrane potentials between −40 and 40 mV. The depolarizing pulse duration was 50 ms and pulses were applied every 5 s. The fraction of unblocked current (I/I_0) is plotted against CTX concentration. The solid curve is drawn according to the equation $I/I_0 = [1 + ([CTX]/K_i]^{-1}$ with $K_i = 4$ n*M*. Four site-specific mutant channels (indicated on figure) are blocked by CTX with the same affinity as the wild-type *Shaker* B channel. The mutations involve the seven acidic residues indicated in the first two outer loops of Fig. 1. Each point for wild-type, EE333,334QQ, or EE268,269QQ represents the mean of measurements on two or three separate oocytes; the range of these determinations was smaller than the size of the point. Each point for ED335,336QN and D274Q was measured in a single oocyte. *Xenopus* oocytes were prepared and injected with in vitro transcript as described (*8*) with wild-type and mutated *Shaker* H4 (*15*), which is identical to *Shaker* B (*13*). Site-specific mutations were introduced into *Shaker* H4 inserted into Bluescript plasmid (Stratagene) by the method of Kunkel (*22*), and mutant clones were selected by DNA sequencing. K^+ currents (typically 1 to 4 μA) were recorded with a two-electrode voltage clamp (Almost Perfect Electronics) 2 to 4 days after the injection of transcript and were analyzed with a laboratory computer. The recording chamber was continuously perfused with a low Ca^{2+} saline to minimize the endogenous Ca^{2+}-activated Cl^- currents (*23*). The composition of the saline was 96 m*M* NaCl, 2 m*M* KCl, 0.3 m*M* $CaCl_2$, 1 m*M* $MgCl_2$, 5 m*M* Hepes (*p*H 7.6) with or without CTX. CTX was purified from *L. quinquestriatus* venom (*5*).

In contrast to the negative results of mutations on the first two outer loops, we identified a residue in the third external loop that did affect CTX block: Glu^{422}. K^+ currents measured in oocytes injected with mRNA coding for either wild-type K^+ channels or for two point mutants, E422Q and E422K, in which the negatively charged Glu^{422} is changed to a neutral glutamine or a positive lysine are shown in Fig. 3. The K^+ currents are identical with respect to voltage-dependent kinetics of activation and inactivation; however, the wild-type channel is more sensitive to CTX than either of the mutants. Addition of 8 n*M* CTX inhibits wild-type currents by 70%, but reduces the glutamine and lysine mutants by only 40% and 15%, respectively. For each of these mutations, we assayed two independently chosen clones and observed identically altered CTX inhibition.

In the absence of structural information, mutagenesis experiments must be interpreted with caution, since a mutation in one region of a protein may result in far-reaching conformational changes. Although the structure of this K^+ channel is unknown, we are nevertheless in a position to ask whether the effects of these mutations are direct and local and to test a specific mechanism by which the mutations affect CTX block. In analogy to mechanistic work on CTX interaction with a related K^+ channel (*5, 12*), we suggest that the mouth of this channel carries negative charges located close to but not at the toxin binding site. These charges would attract the highly basic CTX molecule toward its binding site by establishing a local negative electrostatic potential in the vicinity of the site. This "electrostatic focusing" mechanism makes a quantitative prediction about the effects of charge mutations. Suppose that ψ is the local potential at the CTX binding site; this potential is determined by the position of all the charges on the channel protein, as well as the geometry of the system, and is therefore unknown. If a mutation is made that alters a charge by one unit, then the potential at the binding site will change by a value $\Delta\psi$. As a result of this altered potential, the binding energy of the toxin, and hence its measured inhibition constant, will change according to:

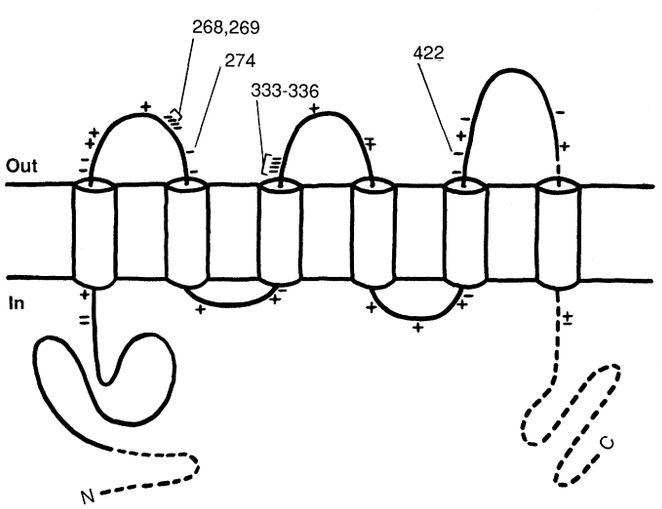

Fig. 1. Transmembrane folding model for a *Shaker* K^+ channel. This model represents a consensus cartoon of several proposals based on the hydropathy profile of the *Shaker* K^+ channel (*10, 11*). There are six membrane-spanning regions, and the termini are assumed to be cytoplasmic. The dashed segments correspond to the variable regions of the different Shaker splicing variants (*13*). We indicate the approximate position of every charged residue in the linkers connecting the transmembrane segments, as well as the residue numbers of site-directed mutants produced in this study.

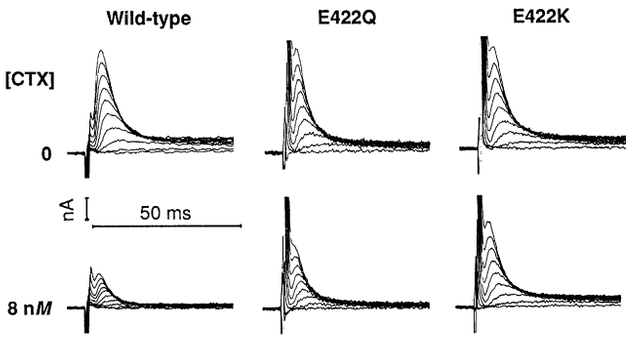

Fig. 3. Mutations at position 422 influence the binding of CTX. K^+ currents were measured in oocytes 3 days after the injection of transcript from *Shaker* B wild-type cDNA and two point mutants. The mutations replace the wild-type Glu^{422} with a glutamine (E422Q) or lysine (E422K). The membrane potential was held at −100 mV and stepped to test potentials between −40 and +40 mV in 10-mV increments, as in Fig. 2. Currents measured are shown before and after the addition of 8 n*M* CTX. Inhibition by CTX was fully reversed by 20 min of perfusion in normal saline. Current amplitude scale bar is 1000, 250, and 330 nA for wild type, E422Q, and E422K, respectively.

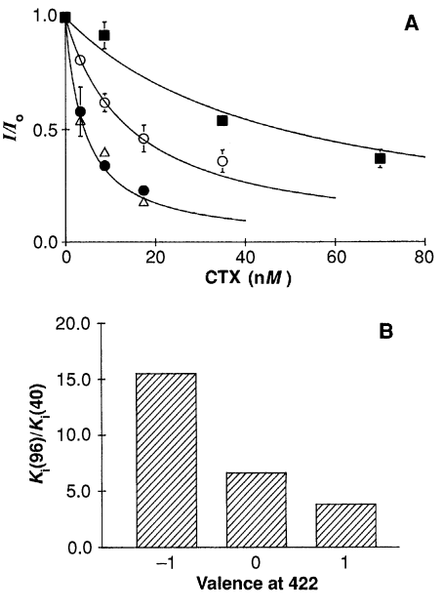

Fig. 4. (**A**) CTX affinity is a simple function of the charge at position 422. CTX inhibition of K^+ currents was measured as in Fig. 2. Inhibition curves for wild-type Shaker B and three mutants involving residue 422 are shown. Glutamate-422 was replaced by either glutamine (E422Q), lysine (E422K), or aspartate (E422D). Solid curves correspond to inhibition constants of 4.2 n*M* for the wild-type (●) and E422D (△), 14.5 n*M* for E422Q (○), and 48 n*M* for E422K (■). Each point represents the mean ± SEM of two to six determinations, each in a different oocyte. (**B**) Ionic strength dependence of CTX block is weakened as negative charge is reduced at residue 422. The inhibition constant for CTX was determined for wild-type, E422Q, and E422K channels (corresponding to a valence at 422 of −1, 0, and +1, respectively) in the standard assay solution containing 96 m*M* NaCl and then after reducing the NaCl to 40 m*M*, maintaining osmolarity with sucrose. The ratio of inhibition constants $[K_i(96)/K_i(40)]$ is plotted as a function of the valence at residue 422. At high salt, each K_i was determined at four to five CTX concentrations in two to six oocytes; at low salt, each K_i was determined at three to four CTX concentrations in a single oocyte. K_i values are reproducible within ±20% of the mean value.

$$K'/K = \exp(zF\Delta\psi/RT) \quad (1)$$

where K and K' are the inhibition constants before and after the charge alteration, and z is the effective valence of the toxin. Furthermore, if the sole effect of changing charged residues is on the local electrostatic potential, it follows that if a mutant is made that changes the residue charge by two units (that is, glutamate to lysine) then the resulting inhibition constant, K'', should be given by the square of the effect of changing the residue by a single unit (that is, glutamate to glutamine):

$$K''/K = [K'/K]^2 \quad (2)$$

This argument can be generalized to show that the conclusion is valid even if the toxin is not considered a point charge but rather an array of charges distributed in space, as is in fact the case.

This electrostatic model accounts quantitatively for our observations on the mutations at position 422. CTX inhibition curves were measured for wild-type channels and several electrostatic mutants (Fig. 4). The half-inhibition concentration (K_i) for the wild-type channel is 4.2 n*M* and for the single-charge mutant E422Q, 14.5 n*M*. If this weakening of binding affinity is purely electrostatic, Eq. 2 predicts that the lysine mutant, E422K, should display a K_i of 50 n*M*. This prediction is in agreement with the K_i of 48 n*M* observed for this mutant, and its validation provides strong support for the idea that these mutations are operating locally near the binding site by a simple electrostatic mechanism. This result is entirely consistent with electric field superposition in the vicinity of the CTX binding site; additivity of fields is expected as long as the charge density, and thus the electric potential, is small.

A further argument for an electrostatic effect of these mutations emerges from the complete absence of an effect on CTX binding in the aspartate mutant E422D, in which the negative charge at position 422 is preserved. If the residue at 422 were directly involved in an intimate interaction with toxin right at the binding site, we might expect to observe a substantial effect on the binding affinity when the structure of this site is altered by shortening the side chain.

Any through-space electrostatic interaction should be sensitive to the ionic strength of the aqueous medium in a qualitatively predictable way. Since the positively charged toxin experiences a local net negative potential at its binding site, CTX block should weaken as ionic strength is raised and attractive electrostatic forces are concomitantly reduced. Furthermore, as the net charge of the channel is made less negative, the toxin affinity should become less sensitive to ionic strength (*12, 17*). This additional expectation is borne out by experiment (Fig. 4B). Here, we examine CTX inhibition at two ionic strengths, for wild-type and charge-mutated channels. In all three cases, raising ionic strength lowers the affinity of CTX block. But this effect is reduced as the charge at position 422 is varied in the positive direction. This result provides an independent, though qualitative, support for the electrostatic mechanism under consideration here.

This study shows that Glu^{422} of the *Shaker* B K^+ channel stabilizes the binding of CTX by exerting a purely electrostatic influence on the cationic toxin. There are several well-documented cases for which an electrostatic mechanism, operating over distances of 5 to 15 Å, influences the affinity of a charged ligand binding to a protein. Negatively charged residues that are near but not at the Ca^{2+} binding sites of calbindin (*18*) and subtilisin (*19*) enhance the binding affinity of Ca^{2+}. Similarly, negative charges located outside of the active site of subtilisin perturb the pK_a of the active site histidine by a simple electrostatic effect (*20*). In an analogous way, surface charges on Zn, Cu superoxide dismutase enhance the diffusion-limited association rate of the superoxide anion (*21*). These examples involving known protein structures provide clear precedents for the importance of long-range electrostatic forces in ion binding.

The electric potential due to a source charge (that is, a charged amino acid side chain) decreases with distance from the charge. Our experiments show that a single charge alteration on the channel reduces the CTX affinity 3.5-fold, equivalent to a free energy change of about 3 kJ/mol. Because the net valence of CTX is known, we should be able in principle to determine the distance between position 422 and the CTX binding site. However, several unknown factors make such an estimate uncertain. First, we do not know precisely how the

electric potential varies with distance, since this is affected by the local geometry and charge distribution of the protein-solution dielectric interface. Second, CTX is not a point charge, but rather a protein with a spatial distribution of charges. Finally, the total charge alteration resulting from a single point mutation depends on an unknown number of polypeptide chains making up the oligomeric channel complex. In spite of these uncertainties, it is instructive to make some plausible assumptions and calculate the distance from Glu^{422} to the CTX binding site. We use Debye-Huckel theory to approximate the electric potential variation with distance from a point charge, and we assume an effective valence of +5 for CTX. Then, considering that the local electric fields are mainly confined to aqueous regions of dielectric constant 80, we calculate a distance of 17 Å between position 422 and the CTX binding site, for a homotetrameric channel. Although this is a very crude estimate, it is a plausible one, falling squarely within the range of distances over which electrostatic focusing mechanisms operate in cases of known macromolecular structures (*18–21*).

These results have identified the physical mechanism by which Glu^{422} influences CTX binding energy in the outer mouth of the *Shaker* K^+ channel: via the electrostatic potential arising from surface charges some 10 to 20 Å distant from the toxin binding site. The effect of Glu^{422} is therefore local, and so we conclude that position 422 of the *Shaker* K^+ channel must reside on the extracellular side of the membrane. This information is in harmony with the standard folding models of this channel (*10, 11*), and it places a strong constraint upon more refined models of this transmembrane folding topology. Moreover, it localizes a region of the channel sequence near the external ion entryway. This region can be used as a starting point for future efforts to identify amino acid residues directly involved in the binding of the toxin, and, eventually, in the ionic conduction process itself.

REFERENCES AND NOTES

1. E. Moczydlowski, K. Lucchesi, A. Ravindran, *J. Membr. Biol.* **105**, 95 (1988).
2. A. Hermann and C. Erxleben, *J. Gen. Physiol.* **90**, 27 (1987).
3. D. Wolff, X. Cecchi, A. Spalvins, M. Canessa, *J. Membr. Biol.* **106**, 243 (1988).
4. R. S. Lewis and M. D. Cahalan, *Science* **239**, 771 (1988).
5. C. Anderson, R. MacKinnon, C. Smith, C. Miller, *J. Gen. Physiol.* **91**, 317 (1988).
6. R. MacKinnon and C. Miller, *ibid.*, p. 335.
7. C. Miller, *Neuron* **1**, 1003 (1988).
8. R. MacKinnon, P. Reinhart, M. M. White, *ibid.*, p. 997.
9. D. M. Papazian, T. L. Schwarz, B. L Tempel, Y. N. Jan, L. Y. Jan, *Science* **237**, 749 (1987); A. Kamb, L. E. Iverson, M. A. Tanouye, *Cell* **50**, 405 (1987); A. Baumann *et al.*, *EMBO J.* **6**, 3419 (1987).
10. W. A. Catterall, *Science* **242**, 50 (1988).
11. B. L Tempel, D. M. Papazian, T. L. Schwarz, Y. N. Jan, L. Y. Jan, *ibid.* **237**, 770 (1987); H. R. Guy, in: *Monovalent Cations in Biological Systems*, C. A. Pasternak, Ed. (CRC Press, Cleveland, OH, in press).
12. R. MacKinnon, R. Latorre, C. Miller, *Biochemistry*, in press.
13. T. L. Schwarz, B. L Tempel, D. M. Papazian, Y. N. Jan, L. Y. Jan, *Nature* **331**, 137 (1988).
14. L. C. Timpe, Y. N. Jan, L. Y. Jan, *Neuron* **1**, 659 (1988); O. Pongs *et al.*, *EMBO J.* 7, 1087 (1988).
15. A. Kamb, J. Tseng-Crank, M. A. Tanouye, *Neuron* **1**, 421 (1988).
16. R. MacKinnon and C. Miller, unpublished observation.
17. ———, *Biochemistry*, in press.
18. S. Linse *et al.*, *Nature* **335**, 651 (1988).
19. M. W. Pantoliano *et al.*, *Biochemistry* **27**, 8311 (1988).
20. A. J. Russell and A. R. Fersht, *Nature* **328**, 496 (1987).
21. E. D. Getzoff *et al.*, *ibid.* **306**, 287 (1983); K. Sharp, R. Fine, B. Honig, *Science* **236**, 1460 (1987).
22. T. A. Kunkel, *Methods Enzymol.* **154**, 367 (1987).
23. M. E. Barish, *J. Physiol. (London)* **342**, 309 (1983).

24. We thank L. Y. Jan and Y. N. Jan for providing *Shaker* clones A, B, C, and D; M. Tanouye for the *Shaker* H4 clone; S. Friedman, R. Leonard, and D. Oprian for advice and guidance on recombinant DNA methods. Supported by NIH research grants AR 19826 and GM 31768, and by NIH training grant NS 07292.

25 April 1989; accepted 21 July 1989

Long-Term Potentiation in the Motor Cortex

ATSUSHI IRIKI, CONSTANTINE PAVLIDES, ASAF KELLER, HIROSHI ASANUMA

Long-term potentiation (LTP) is a model for learning and memory processes. Tetanic stimulation of the sensory cortex produces LTP in motor cortical neurons, whereas tetanization of the ventrolateral nucleus of the thalamus, which also projects to the motor cortex, does not. However, after simultaneous high-frequency stimulation of both the sensory cortex and the ventrolateral nucleus of the thalamus, LTP of thalamic input to motor cortical neurons is induced. This associative LTP occurs only in neurons in the superficial layers of the motor cortex that receive monosynaptic input from both the sensory cortex and the ventrolateral nucleus of the thalamus. Associative LTP in the motor cortex may constitute a basis for the retention of motor skills.

IT IS GENERALLY BELIEVED THAT learning and memory processes are subserved by some form of synaptic plasticity within the central nervous system. Long-term potentiation (LTP), that is, the long-lasting enhancement of synaptic transmission, occurs in the hippocampus (*1*), and this LTP is thought to participate in mnemonic processes for cognitive events (*2*). However, in humans learning and retention of motor skills are subserved by other areas of the brain (*3*), perhaps in the motor cortex (MCx) (*4*) and/or in the cerebellum (*5*).

We have recently demonstrated that tetanic stimulation of the sensory cortex (SCx) can induce LTP in motor cortical neurons (*6*), which suggests that the corticocortical (CC) input from the SCx to the MCx is involved in the acquisition of motor skills. In that study, tetanic stimulation of the ventrolateral nucleus of the thalamus (VL) never produced homosynaptic LTP in motor cortical neurons (7), and this has been confirmed in many cells in the present experiment. Furthermore, when a motor cortical neuron received short-latency excitatory postsynaptic potentials (EPSPs) from both the SCx and the VL, tetanic stimulation of the SCx produced homosynaptic LTP in SCx input but did not produce heterosynaptic LTP in VL input (five cells) (*6*), suggesting that VL input is not related to motor learning. However, elimination of CC input to the MCx in the cat produces retardation in learning motor skills, but elimination of CC input after the learning does not eliminate previously acquired motor skills (*8*). This observation suggests that, in addition to the synaptic plasticity in the CC pathway, there are plastic processes in some additional pathways projecting to the motor cortex. Simultaneous tetanic stimulation of two inputs in the hippocampus, one of which does and the other of which does not produce LTP, can produce associative LTP in the latter input (*9*). We now report that associative LTP can also be induced in the thalamic input to the MCx by combined tetanic stimulation of the SCx and the VL.

Results were obtained from 14 young adult cats anesthetized with Nembutal. Five platinum-in-glass microelectrodes were implanted in the SCx (area 2), and four metal electrodes were placed in the VL for microstimulation. Intracellular recordings were made from neurons in the MCx (area 4) with a glass microelectrode filled with 3*M* KCl and a double-barreled, closed chamber technique (*10*). Stable intracellular recordings were obtained from more than 500 cortical neurons. Of these, 18 neurons that

Rockefeller University, New York, NY 10021.